Journal of Applied Polymer Science

Characterization of Polyhydroxybutyrate Biosynthesized from Crude Glycerol Waste Using Mixed Microbial Consortia

Shengjun Hu,[1] Armando Gabriel McDonald,[1] Erik Robert Coats[2]

[1]Department of Forest, Rangeland and Fire Science, Renewable Materials Program, University of Idaho, Moscow, Idaho 83844-1132

[2]Department of Civil Engineering, University of Idaho, Moscow, Idaho 83844-1022

Correspondence to: A. G. McDonald (E-mail: armandm@uidaho.edu)

ABSTRACT: This study focused on the characterization of polyhydroxybutyrate (PHB) produced from crude glycerol (CG) using mixed microbial consortia (MMC). PHB recovered from two biomass drying treatments (65°C oven drying and lyophilization) was characterized comparatively along with a commercially sourced PHB (PHB-C). Characterization results showed that oven-drying method caused PHB partial hydrolysis, as indicated by its lower molecular weight (M_w) (PHB-O, 144,000 g mol^{-1}), which further affected its physical and chemical properties. Lyophilization helped alleviate PHB hydrolysis during drying process, leading to PHB (PHB-L) of higher M_w (309,000 g mol^{-1}) and material properties comparable with commercial PHB. Furthermore, crystallization and morphological studies showed that PHB-L featured faster crystallization rates and smaller spherulites as compared with PHB-C, probably due to its lower M_w. In general, the results from this study suggested that CG-MMC-derived PHB-L possessed material properties comparable with those of pure substrate/culture produced PHB. © 2012 Wiley Periodicals, Inc. J. Appl. Polym. Sci. 129: 1314–1321, 2013

KEYWORDS: biopolymers and renewable polymers; crystallization; mechanical properties; thermal properties; thermoplastics

Received 11 September 2012; accepted 9 November 2012; published online 3 December 2012
DOI: 10.1002/app.38820

INTRODUCTION

Polyhydroxyalkanoates (PHAs) are a family of polyesters that are naturally biosynthesized by a variety of bacteria. To date more than 300 different PHA-producing bacterial species have been isolated.[1,2] PHAs are accumulated as granules within the bacterial cytoplasm as carbon and energy reserves, analogous to starch in plants and to glycogen in bacterial and mammalian systems, under nutrient limited or unbalanced growth conditions.[3,4] PHAs have received extensive research attention because of their similar material properties to and potential replacement of conventional petro-plastics; plus, they are biodegradable, biocompatible, and renewable.[2] The material properties of PHAs are quite versatile, ranging from rigid plastics to elastomers, due to their large number of monomeric constituents.[5] For example, PHAs with monomers containing 3-5 carbon atoms are referred as short-chain-length (SCL) PHAs and include poly (3-hydroxybutyrate) (PHB) and poly (3-hydroxybutyrate-*co*-3-hydroxyvalerate) (PHBV). PHB is generally considered to be rigid and brittle unless they were processed by such special techniques as annealing and drawing.[6] Compared with PHB, PHBV showed more favorable mechanical properties such as improved flexibility and reduced brittleness, although the exact material properties of PHBV largely depend on the content of hydroxyvalerate units in its molecular chains.[7]

While PHA is an attractive renewable alternative to petroleum-based thermoplastics, current commercial production practices exhibit higher production costs than conventional plastics; their higher production costs are largely associated with substrate production and bioreactor operations.[8,9] Research to minimize these impacts has been focusing on the use of pure cultures with waste streams rich in organic carbon[10–13] or mixed microbial consortia (MMC) grown on synthetic feedstocks.[14–16] The use of MMC has great potentials in reducing PHA production costs, principally due to the elimination of requirement to maintain axenic conditions for bioreactor operations.[15,17] Depending on different substrates and feeding conditions, PHA contents in MMC synthesized biomass vary widely from approximately 40–89% dry cell weight, while pure culture synthesized biomass generally shows PHA contents from 75 to 90%.[15,17–22] Generally, the material properties of MMC-derived PHA such as molecular weight and thermal transitions have been shown to be similar to those derived from pure cultures.[20]

Crude glycerol (CG) is a low value byproduct from biodiesel production due to the oversupply and the presence of various impurities such as soap, methanol, fatty acid methyl esters, and glycerides.[23,24] It has been estimated that roughly 1 kg CG is generated per 10 kg of biodiesel produced.[25–27] The recent rapid increase in biodiesel production has created a large surplus of low-value crude glycerol, which has become a financial and environmental liability for the biodiesel industry. The combined use of low-value CG and MMC offers a cost effective alternative to the production of PHA from pure cultures and substrates and could potentially reduce the high polymer production cost.[17] The use of CG as a substrate could also contribute to the cost-effectiveness of the biodiesel industry by value added conversions of its byproduct.

The synthesis of PHB by pure microbial cultures from CG has been previously explored.[13,28,29] The produced PHB exhibited material properties similar to those produced from other common substrates, like acetic acid and glucose, with molecular weights ranging from 620,000 to 960,000 g mol^{-1}.[13,29] While there have been extensive reports on the production of PHA from mixed cultures and/or from waste feedstocks, reports on the characterization of PHA obtained from these practices have been relatively few.[30–32] Among a few available reports, the molecular weight and thermal properties of PHA were mainly discussed, while other aspects of mixed culture derived PHA such as mechanical, viscoelastic, and morphological properties were not explored. In addition, while lyophilization is a well-accepted and used practice for drying biomass before PHA recovery, it presents potentially high capital and operational costs when applied in commercial scales. Other more commonly seen drying methods, such as regular oven drying at modest temperatures (e.g., 50–80°C), have not been reported in literature for PHA biomass drying: particularly their effects on polymer properties. Compared to lyophilization, regular oven drying represents potentially lower capital and operational costs that could contribute to further cost reduction for PHA production.

In this study, we investigated the chemical, thermal, mechanical, and viscoelastic properties of the CG-derived PHB recovered from two biomass drying methods: oven-drying (PHB-O) and lyophilization (PHB-L). PHB material properties were compared with those of a commercial PHB sample. The aim of this study was to (a) provide a perspective on the properties of CG and MMC-derived PHB with regard to its comparison to that of PHB derived from pure substrates and pure cultures; (b) explore the effects of different biomass drying methods on polymer properties to shed some lights on the feasibility of other drying methods alternative to lyophilization.

MATERIALS AND METHODS

Biosynthesis of PHB-Rich Biomass

PHB-rich biomass was biosynthesized in a 12 L bioreactor as previously described.[17] Biomass samples taken from the bioreactor were suspended in 6.25% sodium hypochlorite to lyse the cells[33] and to arrest bacterial metabolic activity during the recovery process. Biomass was centrifuged and the obtained pellet was rinsed with water, lyophilized at −50°C until constant weight (Labconco FreeZone 4.5) and dry cell mass was recorded. To obtain PHB that would be similarly obtained in a commercial system, the biomass was oven dried (and not lyophilized) at 65°C for 16 h prior to extraction and purification. A commercially sourced PHB (PHB-C, T_m = 172°C, Sigma-Aldrich) sample was used as a reference.

PHB Recovery and Purification from PHB-Rich Biomass

Lyophilized or oven dried biomass (of known quantity) was pre-extracted in boiling acetone (20 volumes, 15 min). The acetone extract was discarded, followed by the transfer of biomass to a round bottom flask (250 mL), to which $CHCl_3$ was added (50 volumes). The biomass slurry was then refluxed in boiling $CHCl_3$ under constant stirring overnight (16 h); the obtained $CHCl_3$ extract was separated from the biomass slurry by filtration and concentrated under vacuum. PHB was dissolved in a minimum amount of $CHCl_3$ and then precipitated by addition of five volumes of cold petroleum ether (boiling point range 35–60°C) under constant stirring, centrifuged (3000 rpm, 5 min). The supernatant was discarded after complete settling down of PHB. Then the obtained PHB was vacuum dried to constant weight and the mass of polymer was recorded.

FTIR Spectroscopy

Samples were analyzed by FTIR spectroscopy (Avatar 370 FTIR, ThermoNicolet) using an attenuated total reflectance (ATR) single-bounce ZnSe cell. All spectra were ATR and baseline corrected using the Omnic v7.0 software (ThermoScientific).

Molecular Weight Determination

The weight average molecular weight (M_w) of purified PHB was determined by gel permeation chromatography (GPC). Separation was achieved using a ViscoGEL I-MBHMW-3078 (Viscotek) column at 40°C on elution with either stabilized tetrahydrofuran (THF) or $CHCl_3$ at 1 mL min^{-1} and detected using a triple detection system (refractive index (Waters model 2478), low- and right-angle laser light scattering (LALLS, RALLS), and differential viscometer [Viscotek model 270, Viscotek Corporation)]. Data analysis was performed using OmniSEC 4.1 (Viscotek) software with reference to a narrow polystyrene standard (Viscotek, M_w = 98,946 g mol^{-1}).

Thermal Analysis

Thermal analysis was conducted by differential scanning calorimetry (DSC) on a TA Instrument Q200 device equipped with refrigerated cooling. For the determination of melting temperature (T_m), glass transition temperature (T_g), and degree of crystallinity (X_c), test procedures included first heating the sample to 180°C to destroy any prethermal history, then cooling to −50°C, and finally, reheating to 180°C for the determination of thermal transitions. An equilibration time of 3 min was applied after each heating and cooling cycle at ramping rates ±10°C min^{-1}. The T_m was taken as the peak maximum of the crystallite melting peak. The degree of crystallinity was calculated by dividing fusion enthalpy by 146 J g^{-1} (for 100% crystalline PHB).[34] The T_g was recorded as the inflection point in the thermogram.

For melt-isothermal crystallization kinetics study, samples were rapidly (100°C min^{-1}) heated to 190°C, held for 1.5 min to destroy any nucleation sites, followed by rapid (−50°C min^{-1}) cooling to target isothermal temperatures (105, 110, 115, and 120°C). All samples were held at the isothermal crystallization temperatures for 1 h to allow complete crystallization of PHB. Based on the DSC thermogram, the relative crystallinity, X_t, of

Applied Polymer SCIENCE

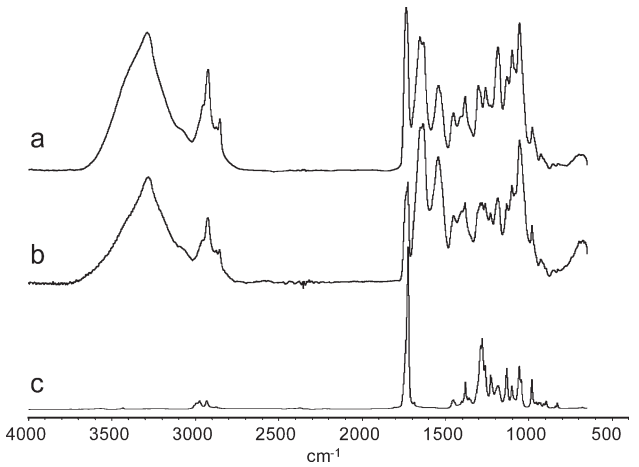

Figure 1. ATR-FTIR spectra of (a) crude biomass, (b) extracted residual biomass and (c) PHB-L.

PHB at time t was calculated from the equation: $X_t = \int_0^t \left(\frac{dH}{dt}\right) dt / \int_0^t \left(\frac{dH}{dt}\right) dt$; the activation energy of crystallization, E, was calculated from the equation: $V_c = A \exp\left(-E/RT_c\right)$, where V_c is the rate of crystallization determined as the slop of the linear region of X_t vs t plot, A is the pre-exponential factor, R is the gas constant, and T_c is the crystallization temperature. The isothermal crystallization kinetics of PHB was analyzed and fitted to the rearranged Avrami equation[35]: $\lg(-\mathrm{In}(1 - X_\downarrow t) = \lg k + n \lg t)$, where X_t, k, n, and t are relative crystallinity, Avrami rate constant, Avrami exponent, and crystallization time, respectively.

Mechanical and Viscoelastic Analysis

PHB films were prepared by $CHCl_3$ solvent casting on Teflon molds, vacuum dried for 24 h and then conditioned (25°C, 50% relative humidity) for 7 days before tensile testing (15 × 4 × 0.06 mm^3) on a dynamic mechanical analyzer (DMA) model Q800 instrument (TA Instruments). Tensile testing was conducted at a constant force of 1 N min^{-1} until break. Tensile strength, Young's modulus, and elongation at break were determined from the constructed stress–strain curve using Universal Analysis software (TA instruments). Viscoelastic analysis of PHB was conducted in the tensile mode with temperature ramping from −50 to 180°C at 3°C min^{-1}, 0.05% strain, and at 1 Hz.

Hot Stage-Polarized Optical Microscopy

Solvent cast PHB films were used for morphological studies on iso-thermally formed crystals using an Olympus BX51 microscope [equipped with 10× objective, polarized light filters and digital camera (Olympus DP70)] coupled to a Mettler Toledo FP900 Thermosystem (FP90 central processor and FP84 microscope) hot stage. Samples were first heated at 20°C min^{-1} to 190°C and then held for 1.5 min to remove any nucleation sites. Samples were then cooled at a rate of −20°C min^{-1} to the desired temperatures (110 and 120°C), followed by isothermal crystallization for 1 h. All images of crystal morphology were processed using the Olympus MicroSuite (TM)-SE 3.2 software.

RESULTS AND DISCUSSION

FTIR Spectroscopic Analysis

FTIR spectroscopy provides fast and powerful identification of functional groups in the biomass and isolated PHB. Using FTIR, Helm and Naumann[36] reported the direct detection and identification of some cell components and functional groups in bacteria. The direct identification of PHB in its producing bacteria and the spectral band assignments for its chemical functional groups have been previously reported.[37,38]

Figure 1 shows the FTIR spectra of crude biomass (i.e., lyophilized biomass before PHB recovery), residual biomass after PHB recovery, and purified PHB (PHB-L) recovered from crude biomass. It can be seen that crude biomass, residual biomass, and PHB-L featured distinctive FTIR spectral profiles associated with their different chemical compositions. The crude biomass spectrum [Figure 1(a)] exhibited dominant bands around 3290, 2900, 1724, 1583, and 1056 cm^{-1}, which can be assigned to OH stretching, C—H stretching, C=O ester stretching, secondary amide (II) and C—OH stretching functional groups, respectively. The peaks around 2900 cm^{-1} and 1583 cm^{-1} suggested the existence of CH containing (aliphatic) compounds and peptides, respectively, which are constituents commonly seen in a wide range of cells.[36] The bands at 3290 cm^{-1} and 1056 cm^{-1} suggested the presence of polysaccharides in the crude biomass. The band at 1724 cm^{-1} in crude biomass indicated the presence of ester linkages, characteristic of PHB. This result agreed well with previous findings that the existence of PHAs can be directly detected and identified in microbial biomass (cells) by FTIR spectroscopy.[36,39] The spectrum of residual biomass showed bands similar to that of crude biomass [Figure 1(b)] together with the PHB ester band suggesting that not all the PHB was extracted and recovered from the biomass. In contrast to the spectrum of crude biomass, the spectrum of PHB-L [Figure 1(c)] showed no characteristic bands associated with hydroxyl (3290 cm^{-1}) and amide (1583 cm^{-1}) groups, confirming that polypeptide and hydroxyl containing compounds (such as polysaccharides) were essentially removed by the PHB recovery/purification process. The ester linkages of PHB, as expected, showed a strong absorbance band around 1724 cm^{-1}. Furthermore, small C—H anti-symmetric stretching bands were observed at 2933, 2977 and 2998 cm^{-1}, which were associated with the methyl side groups of PHB.[40]

Molecular Weight and Thermal Properties of PHB

The M_w of polymers largely affects its material properties, such as viscosity and mechanical strength.[41] The M_w of PHB biosynthesized from CG was monitored over a month bioreactor operational period. As shown in Figure 2(a), the M_w of PHB-L ranged between 200,000 and 380,000 g mol^{-1}, while the M_w of PHB from oven-dried biomass (PHB-O) ranged between 83,400 and 195,000 g mol^{-1}. A statistical analysis showed that the M_w of PHB from two drying treatments were significantly different from each other ($P < 0.05$), indicating that the M_w of PHB is sensitive to biomass drying conditions and that partial hydrolysis can occur during oven-drying. Mothes et al.[29] (620,000-750,000 g mol^{-1}) and Cavalheiro et al.[13] (790,000–960,000 g mol^{-1}) reported higher M_w of PHB from CG using pure

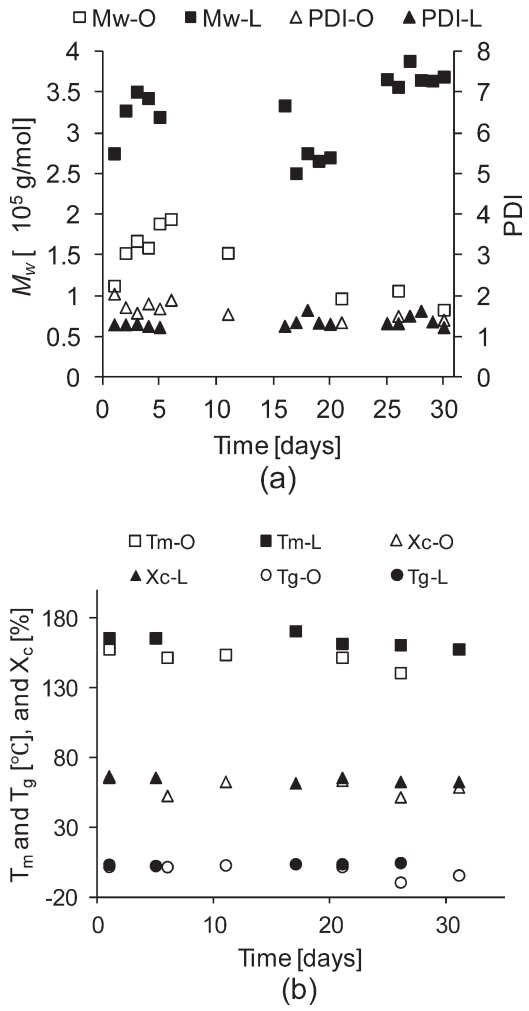

Figure 2. (a) Graph of M_w and PDI of PHB-L (M_w-L and PDI-L) and PHB-O (M_w-O and PDI-O) samples taken over a 30-day period from the bioreactor, (b) Graph of thermal properties of PHB-O (T_m-O, T_g-O, and X_c-O) and PHB-L (T_m-L, T_g-L, and X_c-L) samples taken over a 32-day period from the bioreactor.

microbial cultures, namely *P. denitrificans*, *C. necator JMP 134*, and *C. necator DSM 545*. The observed differences were most likely a result of different microbial communities (i.e., MMC versus pure cultures) and different feeding conditions.[4] It has been reported that the molecular weights of PHA, obtained from both pure and mixed cultures, are sensitive to various operational conditions, namely cultures, feeding conditions, substrates, and so on.[10,20] Thus, it is of vital importance to optimize process conditions to produce PHA with desirable molecular weights. As a reference, the M_w of the commercial PHB (PHB-C) used in this study was determined to be 437,000 g mol^{-1}. Figure 2(a) also shows that the polydispersity index (PDI) of PHB-L ranged between 1.2 and 1.7, slightly lower than that of PHB-O ranging between 1.3 and 2.1. The higher PDI of PHB-O indicates it has a wider M_w distribution, most likely due to the random scission/degradation of polymer chains during oven drying. Generally, the PDI of PHB obtained in this study are lower than those reported by Mothes et al. (2.6–3.7)[29] and Cavalheiro et al. (3.66),[13] who studied the synthesis of PHB from CG by pure cultures. Similarly, this difference might be caused by different operational conditions and microbial communities involved in different studies.

The thermal properties (T_m, T_g, and X_c) of semicrystalline PHB were determined by DSC over a one month period [concurrent with the M_w investigations discussed above, see Figure 2(b)]. The T_m, T_g, and X_c of PHB-L ranged between 158 and 171°C, 2.8 and 4.9°C, and 62 and 66%, respectively. These properties were comparable to literature values for PHB[32,42] and were also similar to that of PHB-C (T_m: 170°C, T_g: 5.1°C, and X_c: 62%). In contrast, the T_m, T_g, and X_c of the partially hydrolyzed PHB-O ranged between 141 and 158°C, –9.0 and 3.2°C, and 53 and 67%, respectively. It can be seen that PHB-O in general showed larger variations in thermal properties as compared with PHB-L, probably due to the varying of M_w and PDI caused by oven drying. In addition, PHB-L also in general showed higher T_m and T_g than that of the partially-hydrolyzed PHB-O, most likely resulted from its higher M_w. This finding agreed well with a previous report by Reis et al.,[20] who summarized and compared the properties of PHA obtained from pure and mixed cultures. Their results also suggested a trend of increasing T_m and T_g of PHA with increasing M_w. A statistical analysis of the data indicates that T_m of PHB from the two different treatments were significantly different ($P < 0.05$). This indicates that the thermal properties of PHB, particularly T_m, can be affected significantly by the applied biomass drying methods due to their effects on the M_w of PHB. Therefore, in practice oven-drying biomass should be largely avoided if obtaining polymers of high thermal stability is of primary interest.

Tensile and Viscoelastic Properties of PHB

The tensile properties of solvent-cast PHB films were determined. Their typical stress–strain curves are shown in Figure 3. The tensile strength and Young's modulus of PHB-L were 14 MPa (CoV 10%) and 1.8 GPa (CoV 26%), respectively, which were lower than that of PHB-C [tensile strength: 20 MPa (CoV 25%); Young's modulus: 2.3 GPa (CoV 29%)]. This is most likely due to the lower M_w (309,000 g mol^{-1}) of PHB-L as compared with that of PHB-C (437,000 g mol^{-1}). However, the tensile strength of CG-based PHB-L was comparable with those

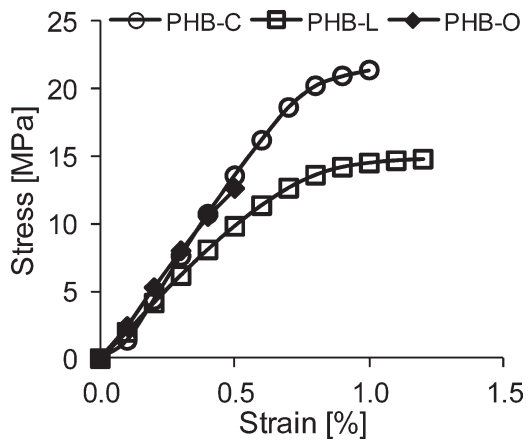

Figure 3. Tensile stress-strain curves for PHB-C, PHB-L, and PHB-O samples.

Applied Polymer SCIENCE

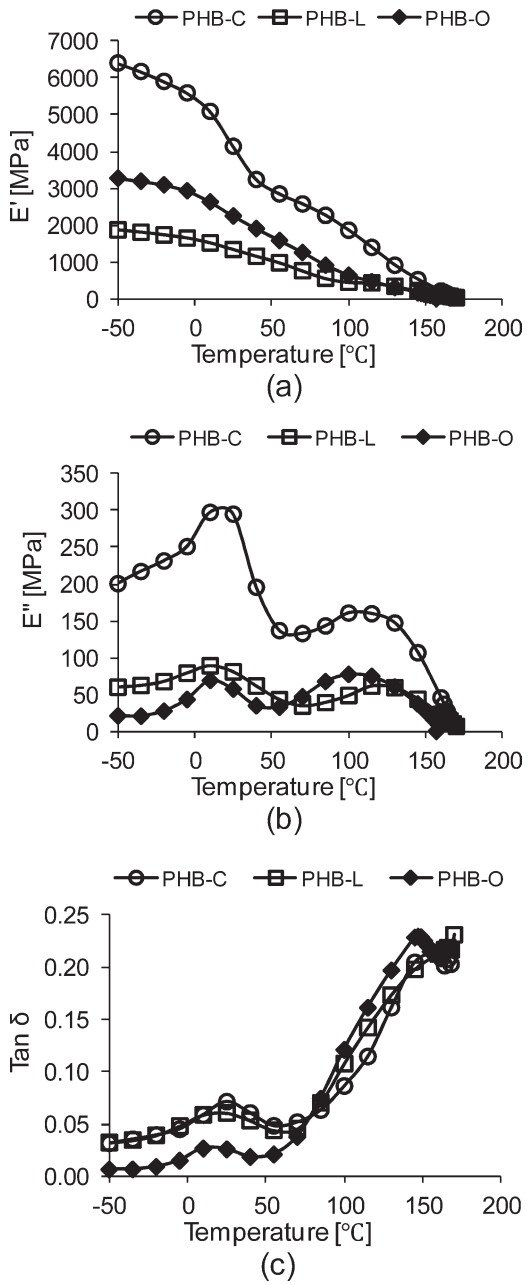

Figure 4. (a) Thermograms of storage modulus (E') for PHB-C, PHB-L, and PHB-O samples, (b) Thermograms of loss modulus (E'') of PHB-C, PHB-L and PHB-O samples, and (c) Thermograms of tan δ of PHB-C, PHB-O and PHB-L samples.

reported by Thellen et al.[43] at 14–16 MPa, who studied the processing and characterization of several commercial PHAs (PHB and PHBV). The Young's modulus and elongation at break (1.3%, CoV 8%) values obtained were also similar to literature values for commercial PHB derived from pure cultures and pure substrates.[43,44] As shown in Figure 3, PHB-O exhibited very similar tensile strength (14.1 MPa, CoV 9%) to that of PHB-L while its Young's modulus of 2.5 GPa (CoV 11%) was higher than that of PHB-L. However, the elongation at break for PHB-O (0.6%, CoV 12%) was much lower than that of PHB-L, indicating it was more brittle under tension probably due to its lower M_w (144,000 g mol^{-1}).

The viscoelastic properties including storage modulus (E'), loss modulus (E'') and damping factor (tan δ) of PHB were determined by DMA. The E' of PHB as a function of temperature is shown in Figure 4(a). For all PHB samples, E' decreased with the increase of temperature. For PHB-C, a steep decrease in E' between 5 and 15°C can be attributed to the glass transition of the amorphous component of the semicrystalline polymer.[45,46] Compared with PHB-C, PHB-O, and PHB-L showed less dramatic glass transition between 0 and 20 °C. The E' of PHB-L and PHB-O at −50°C were 2.0 and 3.4 GPa, respectively, while PHB-C had a much higher E' (6.5 GPa) due to its higher M_w.

The E'' of PHB as a function of temperature is shown in Figure 4(b). The loss modulus at −50°C for PHB-O, PHB-L, and PHB-C were respectively 25, 60, and 200 MPa. The T_g of PHB-C, PHB-L, and PHB-O were determined from the E'' peak maxima, respectively at 19, 15, and 12°C. The T_g determined by DMA differ by several °C than those by DSC because of the different heating rates (10 versus 3°C min^{-1}), thermal history, and testing conditions involved.[47] Thellen et al.[43] reported T_g of different PHB samples ranging between 18.8 and 22.4°C. Compared to PHB-C, CG-based PHB-L, and PHB-O featured slightly lower T_g, probably due to its lower M_w. For all PHB samples, a second E'' maxima was observed between 100 and 120°C, which could be attributed to the start of melt flow.[46]

Figure 4(c) shows the damping factor, tan δ as a function of temperature for the PHB samples. For all samples, tan δ gradually increased with increasing temperature, suggesting that the viscous component of PHB increased as temperature increased. PHB-L exhibited very similar damping behavior to that of PHB-C, while PHB-O had a lower tan δ value (lower proportion of viscous component) in the temperature range of −50 to 80°C. This observation explains partially the brittleness (low elongation %) of PHB-O than other two PHB samples. Above 80°C, an opposite phenomenon was observed, i.e., PHB-O featured higher proportion of viscous component than other two PHB samples, indicating an ease to flow at high temperatures due to its low M_w. The mechanical characterization of PHB with different molecular weights showed that both the tensile and viscoelastic properties of PHB films were highly dependent on their M_w.

Isothermal Crystallization Kinetics

Crystallization is a very important process for any polymer processing. The behavior and/or kinetics of crystallization largely affect the formed polymer structures and thus their final material properties. Therefore, in this study, the isothermal crystallization kinetics of PHB-L was studied at different temperatures and compared to that of PHB-C. Figure 5(a) shows that the crystallization evolution (X_t vs. t) of PHB-L and PHB-C at 110 and 120°C. Isothermal crystallization parameters including crystallization rate (V_c), crystallization half time ($t_{1/2}$), and activation energy were determined (Table I).The crystallization rates of both PHB-L and PHB-C decreased with temperature from 105 to 120°C, leading to the increase of $t_{1/2}$ and the overall time required for the completion of crystallization. Compared with PHB-C, PHB-L showed higher crystallization

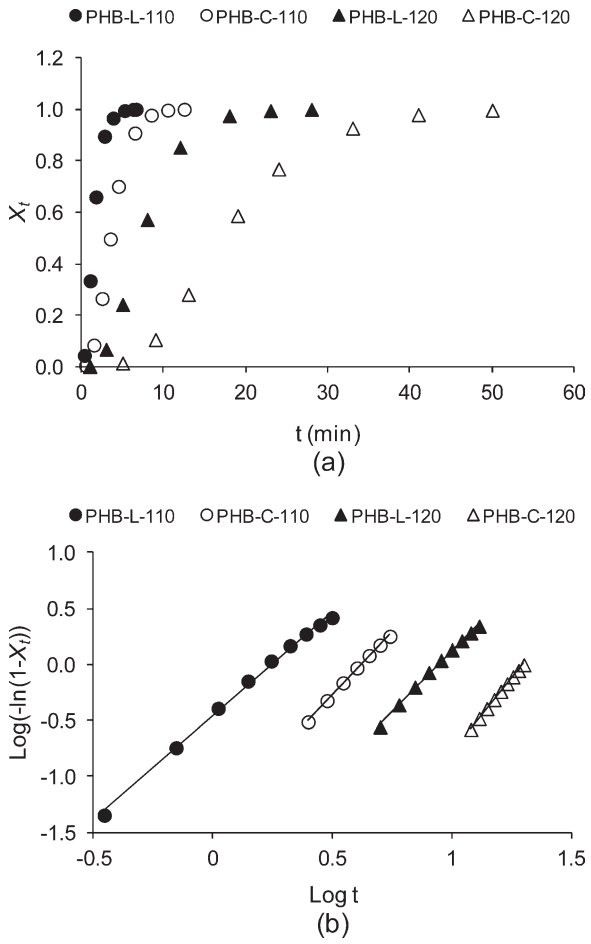

Figure 5. (a) Plot of PHB-L and PHB-C relative crystallinity, X_t, versus time, t, at 110 and 120°C as determined by DSC and (b) Plot of log [-ln (1-X_t)] versus log t at 110 and 120°C for PHB-L and PHB-C as determined by DSC.

rates (V_c) and lower crystallization half time, $t_{1/2}$, at all crystallization temperatures due to its lower M_w. The activation energy for the crystallization of PHB-L and PHB-C were determined to be 136 and 164 kJ mol^{-1}, respectively. Gunaratne and Shanks[35] studied the isothermal crystallization kinetics of PHB (M_w: 230,000 g mol^{-1}) at the same temperature range, and the activation energy of PHB was determined to be 87 kJ mol^{-1}. The observed differences might be due to their contrasting M_w, as higher energy barrier was encountered by longer polymer chains during the course of crystallization.

The Avrami equation has been widely used in studying the isothermal kinetics of various polymer and its suitability in describing the crystallization kinetics of PHAs have been previously demonstrated.[35,48] In this study, experimental data was fitted to the Avrami equation by plotting log(-*ln* (1-X_t)) versus log$t$ at different crystallization temperatures (T_c) (105, 110, 115, and 120°C). Figure 9 shows the Avrami plots of PHB-L and PHB-C at 110 and 120°C. For both samples experimental data fit well with the Avrami equation at 110 and 120°C. Plots at 105 and 115°C also fit well the Avrami equation (data not shown). Avrami parameters, n and k, determined from the

Table I. Crystallization rate (V_c), Crystallization Half Time ($t_{1/2}$), and Activation Energy (E) for PHB-L and PHB-C at Different Temperatures

	PHB-L			PHB-C		
T_c (°C)	V_c (min^{-1})	$t_{1/2}$ (min)	E (kJ mol^{-1})	V_c (min^{-1})	$t_{1/2}$ (min)	E (kJ mol^{-1})
105	0.55	1.13	136	0.37	1.96	164
110	0.44	1.43		0.21	3.51	
115	0.23	2.71		0.11	7.38	
120	0.11	7.43		0.05	17.19	

Avrami plots are listed in Table II. For isothermal crystallization of PHB, both n and k depend on the nucleation mechanism as well as growth geometry.[48] Data as summarized in Table II shows that for both samples the overall rate constant k decreased with temperature increasing, which indicates that the crystallization process occurred faster at lower temperatures (higher super-cooling) and implies that the crystallization process is nucleation controlled.[35] Similarly, PHB-L showed higher overall crystallization rates than PHB-C at all T_c. The values of Avrami exponent, n, ranged from 2.0 to 2.2 and 2.3 to 2.6 for PHB-L and PHB-C, respectively. Gunaratne and Shanks[35] reported n values ranging from 2.12 to 2.32 for PHB, which are similar to the values obtained in this study. Since n values for both PHB-L and PHB-C were close to 2, it is most likely that the isothermal crystallization of both samples proceeded through a two dimensional spherulite growth with a heterogeneous nucleation mechanism.[35]

Morphological Studies

The morphologies of PHB-L and PHB-C isothermally crystallized from melt at 110 and 120°C were observed by polarized light microscopy. As shown in Figure 6, all spherulites showed characteristic Maltese cross birefringence and concentric banding pattern. Straight boundaries observed for neighboring spherulites for all images indicate a heterogeneous nucleation mechanism,[49] which is in agreement with the results from the kinetics study discussed above. For both samples, the formation of spherulites with larger diameters and banding space at higher temperature (120°C) agrees well with previous studies.[34,50] This also agrees with Gunaratne and Shanks's study[35] that slower crystallization at higher temperature tended to induce larger crystals, while faster crystallization at lower temperatures led to smaller crystals due to increased nucleation density. Compared to PHB-L, PHB-C showed larger crystal sizes at both temperatures (110 and 120°C), probably due to its higher M_w and

Table II. Kinetic Parameters for PHB-L and PHB-C at Different T_c

	PHB-L		PHB-C	
T_c(°C)	n	$k(min^{-n_s})$	n	$k(min^{-n_s})$
105	2.0	0.5011	2.3	0.1263
110	1.9	0.3507	2.2	0.0350
115	2.0	0.1147	2.6	0.0037
120	2.2	0.0122	2.6	0.0003

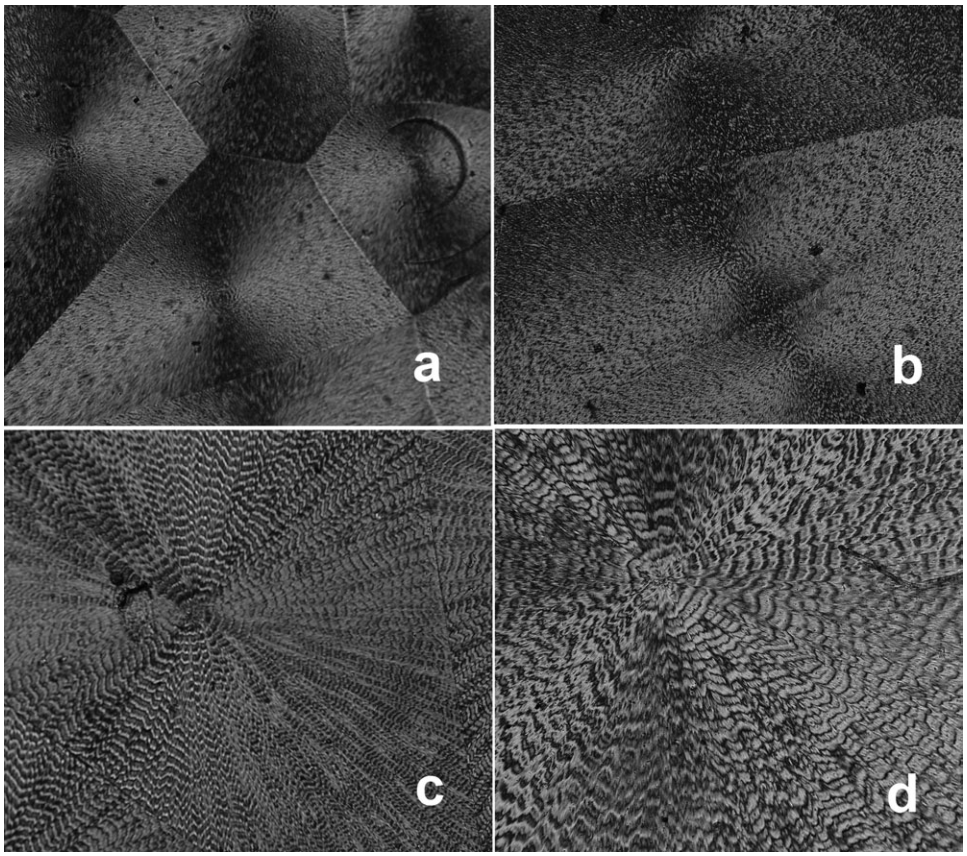

Figure 6. Polarized light micrographs (100×) of crystallized PHB-L: (a) 110°C; (b) 120°C, and PHB-C: (c) 110°C; (d) 120°C.

higher purity.[34] The large crystal size of PHB has long been regarded as one of the main reasons for the brittleness of PHB.[51] Efforts trying to reduce crystal sizes and to alleviate PHB brittleness have been reported.[52] PHB samples produced in this study showed decreased spherulitic radius due to their higher nucleation density that might be beneficial to its mechanical properties.

CONCLUSIONS

In this study, PHB biosynthesized from MMC fed CG was recovered from two biomass drying treatments (oven-drying: PHB-O and lyophilization: PHB-L) and then characterized comparatively with commercial PHB (PHB-C) with regard to their chemical and physical properties. It was found PHB recovered from different biomass drying treatments showed very different material properties, primarily due to the occurrence of partial hydrolysis during the oven-drying process that decreased the molecular weights of PHB. Comparative characterization of PHB-O, PHB-L, and PHB-C showed that molecular weight largely affects the material properties of PHB, particularly its isothermal crystallization kinetics and the crystal morphology; however, MMC-CG derived PHB-L, despite its lower M_w, showed thermal and mechanical properties that are very comparable to that of the commercial PHB made using pure cultures, indicating the potential of producing PHB of promising properties from MMC and CG.

ACKNOWLEDGMENTS

This research was supported by the Western Regional Sun Grant Center at Oregon State University through a grant provided by the US Department of Transportation, RITA under award number DTOS59-07-00055, Sub-Grant Number T0013A-B. The DSC and DMA were supported by a USDA-CSREES grant number 2007-34158-17640. The DSC hot-stage was supported by a USDA-CSREES grant number 2003-35503-13697. The authors would like to acknowledge the technical assistance of Zachary Dobroth and Nicholas Guho for running the bioreactors and collecting samples.

REFERENCES

1. Gross, R. A.; Demello, C.; Lenz, R. W.; Brandl, H.; Fuller, R. C. *Macromolecules* **1989**, *22*, 1106.
2. Dias, J. M. L.; Lemos, P. C.; Serafim, L. S.; Oliveira, C.; Eiroa, M.; Albuquerque, M. G. E.; Ramos, A. M.; Oliveira, R.; Reis, M. A. M. *Macromol. Biosci.* **2006**, *6*, 885.
3. Sudesh, K.; Abe, H.; Doi, Y. *Prog. Polym. Sci.* **2000**, *25*, 1503.
4. van der Walle, G. A.; de Koning, G. J.; Weusthuis, R. A.; Eggink, G. *Adv. Biochem. Eng. Biotechnol.* **2001**, *71*, 263.
5. Philip, S.; Keshavarz, T.; Roy, I. *J. Chem. Technol. Biotechnol.* **2007**, *82*, 233.
6. Aoyagi, Y.; Doi, Y.; Iwata, T. *Polym. Degrad. Stab.* **2003**, *79*, PII S0141–3910(02)00273–2.

7. Keenan, T. M.; Tanenbaum, S. W.; Stipanovic, A. J.; Nakas, J. P. *Biotechnol. Prog.* **2004**, 20.
8. Harding, K. G.; Dennis, J. S.; von Blottnitz, H.; Harrison, S. T. L. *J. Biotechnol.* **2007**, 130.
9. Gerngross, T. U. *Nat. Biotechnol.* **1999**, *17*, 541.
10. Ashby, R. D.; Solaiman, D. K. Y.; Foglia, T. A. *J. Polym. Environ.* **2004**, *12*, 105.
11. Du, G. C.; Yu, J. *Environ. Sci. Technol.* **2002**, *36*, 5511.
12. Braunegg, G.; Genser, K.; Bona, R.; Haage, G.; Schellauf, F.; Winkler, E. *Macromol. Symp.* **1999**, *144*, 375.
13. Cavalheiro, J. M. B. T.; de Almeida, M. C. M. D.; Grandfils, C.; da Fonseca, M. M. R. *Process Biochem.* **2009**, *44*, 509.
14. Beun, J. J.; Paletta, F.; Van Loosdrecht, M. C. M.; Heijnen, J. J. *Biotechnol. Bioeng.* **2000**, *67*, 379.
15. Dionisi, D.; Majone, M.; Papa, V.; Beccari, M. *Biotechnol. Bioeng.* **2004**, *85*, 569.
16. Serafim, L. S.; Lemos, P. C.; Oliveira, R.; Reis, M. A. M. *Biotechnol. Bioeng.* **2004**, *87*, 145.
17. Dobroth, Z. T.; Hu, S.; Coats, E. R.; McDonald, A. G. *Bioresour. Technol.* **2011**, *102*, 3352.
18. Salehizadeh, H.; Van Loosdrecht, M. C. M. *Biotechnol. Adv.* **2004**, 22.
19. Cai, M.; Chua, H.; Zhao, Q.; Shirley, S. N.; Ren, J. *Bioresour. Technol.* **2009**, 100.
20. Reis, M. A. M.; Serafim, L. S.; Lemos, P. C.; Ramos, A. M.; Aguiar, F. R.; Van Loosdrecht, M. C. M. *Bioprocess Biosyst. Eng.* **2003**, 25.
21. Waller, J. L.; Green, P. G.; Loge, F. J. *Bioresour. Technol.* **2012**, *120*, 285.
22. Johnson, K.; Jiang, Y.; Kleerebezem, R.; Muyzer, G.; van Loosdrecht, M. C. M. *Biomacromolecules* **2009**, 10.
23. Santibanez, C.; Teresa Varnero, M.; Bustamante, M. *Chilean J. Agricultural Res.* **2011**, *71*, 469.
24. Hu, S.; Luo, X.; Wan, C.; Li, Y. *J. Agric Food Chem.* **2012**, *60*, 5915.
25. Hu, S.; Wan, C.; Li, Y. *Bioresour. Technol.* **2012**, *103*, 227.
26. Johnson, D. T.; Taconi, K. A. *Environ. Prog.* **2007**, *26*, 338.
27. Thompson, J. C.; He, B. B. *Appl. Eng. Agric.* **2006**, *22*, 261.
28. Ibrahim, M. H. A.; Steinbuechel, A. *Appl. Environ. Microbiol.* **2009**, *75*, 6222.
29. Mothes, G.; Schnorpfeil, C.; Ackermann, J. *Eng. Life Sci.* **2007**, *7*, 475.
30. Serafim, L. S.; Lemos, P. C.; Torres, C.; Reis, M. A. M.; Ramos, A. M. *Macromol. Biosci.* **2008**, 8.
31. Albuquerque, M. G. E.; Martino, V.; Pollet, E.; Averous, L.; Reis, M. A. M. *J. Biotechnol.* **2011**, *151*, 66.
32. Bengtsson, S.; Pisco, A. R.; Johansson, P.; Lemos, P. C.; Reis, M. A. M. *J. Biotechnol.* **2010**, *147*, 172.
33. Berger, E.; Ramsay, B. A.; Ramsay, J. A.; Chavarie, C.; Braunegg, G. *Biotechnol. Tech.* **1989**, *3*, 227.
34. Barham, P. J.; Keller, A.; Otun, E. L.; Holmes, P. A. *J. Mater. Sci.* **1984**, *19*, 2781.
35. Gunaratne, L. M. W. K.; Shanks, R. A. J. *Thermal Analysis Calorimetry* **2006**, *83*, 313.
36. Helm, D.; Naumann, D. *FEMS Microbiol. Lett.* **1995**, *126*, 75.
37. Xu, J.; Guo, B. H.; Yang, R.; Wu, Q.; Chen, G. Q.; Zhang, Z. M. *Polymer* **2002**, *43*, 6893.
38. Bayari, S.; Severcan, F. *J. Mol. Struct.* **2005**, *744*, 529.
39. Hong, K.; Sun, S.; Tian, W.; Chen, G. Q.; Huang, W. *Appl. Microbiol. Biotechnol.* **1999**, *51*, 523.
40. Mayo, D. W.; Miller, F. A.; Hannah, R. W. In Course Notes on the Interpretation of Infrared and Raman Spectra; Wiley: Hoboken, New Jersey, **2004**, p 33.
41. Painter, P. C.; Coleman, M. M. In Essentials of Polymer Science and Engineering; DEStech Publications: Lancaster, PA, **2008**, p 40.
42. Lee, S. Y. *Biotechnol. Bioeng.* **1996**, *49*, 1.
43. Thellen, C.; Coyne, M.; Froio, D.; Auerbach, M.; Wirsen, C.; Ratto, J. A. *J. Polym. Environ.* **2008**, *16*, 1.
44. Dekoning, G. *Can. J. Microbiol.* **1995**, *41*, 303.
45. Singh, S.; Mohanty, A. K. *Compos. Sci. Technol.* **2007**, *67*, 1753.
46. Pederson, E. N.; McChalicher, C. W. J.; Srienc, F. *Biomacromolecules* **2006**, *7*, 1904.
47. Mernard, K. P. Dynamical Mechanical Analysis: A Practical Introduction; CRC Press: Boca Raton, FL, **1999**, p 95.
48. Peng, S. W.; An, Y. X.; Chen, C.; Fei, B.; Zhuang, Y. G.; Dong, L. S. *Eur. Polym. J.* **2003**, *39*, 1475.
49. Wunderlich, B. Thermal Analysis of Polymeric Materials; Springer: Berlin Heidelberg, **2005**, p 910.
50. Xing, P. X.; Dong, L. S.; An, Y. X.; Feng, Z. L.; Avella, M.; Martuscelli, E. *Macromolecules* **1997**, *30*, 2726.
51. Gunaratne, L. M. W. K.; Shanks, R. A. *Eur. Polym. J.* **2005**, *41*, 2980.
52. El-Hadi, A.; Schnabel, R.; Straube, E.; Muller, G.; Henning, S. *Polym. Test.* **2002**, *21*, 665.